Available online at www.sciencedirect.com
ScienceDirect
Journal of Catalysis 250 (2007) 110–120
JOURNAL OF CATALYSIS
www.elsevier.com/locate/jcat

Cu/P(4-PVP) stereochemistry in tetralin liquid-phase oxidation I. Effect of the $CuCl_2$/P(4-PVP) on selectivity

Roberto Galiasso Tailleur [a,*,1], Carlos J. Gómez García [b]

[a] *Instituto de Tecnología Química, Universidad Politécnica de Valencia, Los Naranjos s/n, Valencia, Spain*
[b] *Instituto de Ciencia Molecular, Universidad de Valencia, Pol. La Coma, 46980 Paterna, Valencia, Spain*

Received 12 March 2007; revised 10 April 2007; accepted 16 April 2007

Available online 29 June 2007

Abstract

Cu/P(4-PVP) catalyst was used as catalyst for oxidation of tetralin in liquid phase. The catalyst was prepared by reaction of a Cu(II) salt with a 4-vinylpyridine-co-divinylbenzene polymer receptor and characterized by solid ^{1}H and ^{13}C NMR, XPS, FTIR, ESR spectroscopies, and by chemical reaction with pure tetralin. That information was used to gain insight into the stereochemistry of the active site needed to orient the reaction toward tetralone production. It was found that the Cu coordination with the pyridine was critical in influencing the peroxy-radical catalytic reaction, and that polyvinylpyridine was able to limit the autothermal oxidation. The active center is postulated to be based on a (Cu^{2+}–Cu^{+})-pyridine distorted tetrahedric structure that is modified by the oxireduction reactions with tetralin.

Keywords: Tetralin oxidation; Cu/poly(4-PVP) catalyst; Tetralone; Tetralol; Poly-oxidized compounds

1. Introduction

The search for a selective catalyst to produce oxygenated compounds using air is an interesting field of application [1] in the chemical industry. Systems containing Cu^{2+} nitrogen compounds [2–4], particularly the Cu^{2+}/P(4-PVP) system, have been used for the oxidative coupling of 2,6-dimethylphenol [5]. A review of the potential application of the P(4-PVP) polymer for performing different reactions has been provided by Goe et al. [6]. Modification of the Cu–nitrogen ligand formation and the effect of polymer chain during the amine quaternalization also have been discussed in the literature [7]. But optimization of the stereochemistry of Cu on a P(4-PVP) support for selective oxidation has not been analyzed in depth, which is necessary for designing a more selective oxidation catalyst.

The oxidation of tetralin has been extensively tested as a probe molecule, and it is well known that homogeneously [8] and heterogeneously [9] supported metal compounds catalyze the liquid-phase oxidation of that hydrocarbon. In this way, Brederec et al. [10] reported that for transition metal catalysts, the autooxidation of tetralin was catalyzed by quaternary ammonium. Hronec et al. [11] studied the effect of the type of phenyl amines and showed that the activation/deactivation effects of aromatic amines depend on steric factors and the amine/metal ratio. Mukesh et al. [12] studied the effect of Cu-complexes at a temperature range of 80–100 °C and at an oxygen pressure of 0.5 MPa in an autoclave. Tetralone and tetralol were the major products. These authors found that reactions proceed following two competing parallel radical reactions. The inhibition effect of many compounds, such as polyaromatics and sulfur-containing polyaromatics, also has been reported [13]. Several patents claim the possibility of doing selective oxidation of tetralin to tetralone [14,15], but none has mentioned how to control the secondary and tertiary reactions toward poly-oxidized molecules, leading to light polymer and gum formation. Galiasso Tailleur and Acosta [16] recently measured the kinetics of tetralin oxidation using a Pd α-diimine/silica and proposed two reaction paths for tetralin oxidation: one for thermal and another for catalytic. In general, there is contradictory information about the mechanism of autothermal oxidation of

* Corresponding author.
E-mail address: reg@chemail.tamu.edu (R. Galiasso Tailleur).
[1] TA&M Department Chemical Eng. College Station, TX 77843, USA.

0021-9517/$ – see front matter
doi:10.1016/j.jcat.2007.04.008

tetralin in the presence of metal complexes, and, to the best of our knowledge, there is a lack of understanding about the mechanism of reaction using heterogeneous catalysts. In particular, the role of amines remains unclear, as does the role of free radicals.

The goals of the present work were to promote understanding of the Cu^{2+} stereochemistry on a P(4-PVP) polymer and to selectively perform the liquid-phase oxidation of tetralin used here as a probe molecule. The effect of Cu^{2+} "geometry" on the formation of the peroxy-radical transition state was determined by solid characterization before and after reaction and by testing the active site by the chemical reactions. The influence of different variables was studied to elucidate the mechanism of reaction.

2. Experimental

2.1. Catalyst preparation

The catalysts were prepared by impregnating a poly-4-vinylpyrine (Aldrich) with a $CuCl_2$ solution in different solvents. The polymer was dried at 60 °C for 2 h, after which 10 g of dry polymer was stirred with a solution containing different amount of Cu^{2+} in the selected solvent to make either 2.5, 5, or 10 wt% of Cu in the final catalyst. After 12 h, the solid was filter washed with ethanol and then dried at 60 °C for 2 h. The Cu content sample was designated x% Cu/PVP, where x is the amount of Cu by weight of solid. Another catalyst was prepared by impregnating a hydrotalcite (HT) support [17] with 5% of Cu^{2+} using the same procedure described above, which we designate Cu/HT. The third catalyst used was a commercial $Cu(II)^{-}$ acetate (Aldrich) designated $CuAc_2$. The latter two catalysts were used as reference to compare their selectivity and performance with those of Cu/PVP. All fresh and used catalysts were washed with methanol and vacuum-dried before being characterized.

2.2. Catalyst characterization

The catalyst surface area and pore volume of the dried samples were measured with a Micromeritics 1221 apparatus. The amounts of Cu and N were measured by plasma and acid titration, respectively. The surface properties were evaluated by the following techniques:

2.2.1. FTIR analysis

IR characterization of the (PVP) and Cu/PVP was performed using a Nicolet 750 spectrophotometer. The spectra were obtained in KBr pellets in the region of 3800–400 cm^{-1} with a resolution of 4 cm^{-1} by accumulating 40 scans.

2.2.2. ^{1}H and ^{13}C NMR analysis

Nuclear magnetic resonance spectra of the solid samples were obtained in a Broker 400 spectrometer at room temperature. The 75.47-MHz frequency, with a magic-angle spinning rate of 4 Hz and a CP/MAS technique, was used. The contact time was 3 ms, and the number of scans was 3000.

2.2.3. XPS

X-ray photoelectron spectra were obtained in a Laybous Hereus apparatus (Mg cathode) using 50 eV of power (Ref C_{1s}: 285.0 eV). XPS analysis was used to assess the relative Cu, N, Cl, and O concentrations on the surface using the peak area intensity (corrected). Binding energies were measured, and the Cu, N, and O species were determined by deconvolution.

2.2.4. ESR

Q-band ESR spectra ($\nu = 34$ GHz) were recorded using a Bruker E500 ELEXSYS in the temperature range of 300–4 K. The spectra were measured at 9500–13,500 Gauss with microwave power of 0.06–0.60 mW and modulation amplitudes of 1–3 Gauss. The sweep time was 80 or 160 s.

2.3. Catalytic tetralin oxidation

Pure tetralin (Merck) was oxidized in a semicontinuous isothermal glass stirred tank reactor at atmospheric pressure. First, 10 g of tetralin and 0.8 g of catalyst were placed into the reactor; heated under intense bubbling of air (100 mL/min) to either 80, 90, or 100 °C; and then maintained for 24 h under stirring (300 rpm). Liquid samples were obtained as a function of time and analyzed immediately. The amount of peroxide was determined by the phosphine method [18]. Tetralone and tetralol were measured by gas chromatography (Varian CP3800 with a flame ionization detector) with HP15 methyl silicone in a 25-m, 320-μm column. Quantification was achieved using the internal standard (hexadecane), and the peaks were identified by comparison with pure samples. All of the samples were analyzed immediately.

Previous experiments assessed the effects of stirring, particle size, and gas bubbling on controlling chemical reaction conditions in the reactor. The effect of thermal auto-oxidation has also been analyzed in the presence of poly-4-vinylpyridine (PVP) and silica, and without any solid, at the same operating conditions described above. Catalyst deactivation was checked by recycling the catalyst several times with fresh feed and comparing the tetralin conversion at the same operating conditions. Finally, leaching of Cu was checked by analysis of the liquid product.

3. Results and discussion

3.1. Tetralin oxidation, rate of reaction, and mechanism

3,4-Dihydronaphthalen-1(2H)-one (tetralone–TO) and 1,2,3,4-tetrahydronaphthalen-1-ol (tetralol–TOH) were the main products of 1,2,3,4-tetrahydronaphthalene (tetralin–TH) oxidation, but the reaction proceeded further to produce other soluble compounds that were lumped together and designated low-molecular-weight "polyoxygenates" (Pol). Other insolubles in the reaction product were formed [19] that eventually precipitated. These were determined by Millipore filtration following the ASTM 2274 procedure.

The effect of free radical initiators on the "homogeneous" oxidation of tetralin has been known for some time. According

"Homogeneous" initiation [19]	Heterogeneous initiation
$Cu(Ac)_2$—TH + O_2	$CuCl_2$/(PVP)—TH + O_2
Seeded TOOH	Seeded TOOH
$TOOH + Cu^{2+} \rightarrow TO_2^* + Cu^+ + H^+$	$=ClCuCl + TOOH \rightarrow ClH + =ClCuO + TO$
$TOOH + Cu^+ \rightarrow TO^* + Cu^{2+} + OH^-$	
Propagation	
$TO_2^* + TH \rightarrow TOH + TO^*$	$=ClCuO + TH \rightarrow =ClCu + TOH$
$TO^* + TH \rightarrow TOH + T^*$	$=CuClOH + TOH \rightarrow =ClCu + TO + H_2O$
$TOH + TO^* \rightarrow OTOH + T^*$	$=CuClOO + TH \rightarrow =ClCuO + TOH$
$TOH + TO^* \rightarrow OTO + T^*$	$=ClCuOO + TH \rightarrow =ClCuOH + TO$
	$=ClCuO + TOH \rightarrow OTOH + =ClCu$
$T^* + O_2 \rightarrow TO_2^*$	$=ClCu + O_2 \rightarrow =CuClOO$
Termination	
$TO_2^* + TO_2^* \rightarrow$ inactive products + O_2	$CuClO$ + products $\rightarrow$ (?)

Fig. 1. Proposed mechanism for TH oxidation on Cu/PVP catalyst.

to the classical theory, their effect is to produce a free radical that starts the propagation cycle. Lunak et al. [19], among others, mentioned that the effect of metals (even in traces) is responsible for catalytic decomposition of the peroxide into a free-radical initiator, which starts the propagation cycle. In presence of a homogeneous metal, the peroxide decomposes into a free radical (TO_2^* and TO^*) by reaction to reduce the metal. Then the reaction proceeds through the interaction of the hydrocarbon (TH) with the radical to generate the TO and TOH (Fig. 1, left side). The reoxidized state is obtained again by reaction with O_2. The reaction between the radical and TO or TOH produces the polyoxygenate. The homogeneous reaction is terminated by recombination of the radicals. Tian et al. [20] described the formation of dioxygenates in homogeneous auto-oxidation, but they did not include the formation of more polymerized material formed during the thermal treatment of tetralin. When heterogeneous Cu catalyst is present, the free-radical propagation mechanism is strongly affected, and the survival of a free radical is reduced in the liquid phase.

Based on our results with Pd diimine [9] and the results obtained by Moden et al. for cyclohexane oxidation [21], we propose two parallel reaction paths: thermal auto-oxidation and catalytic conversion of tetralin (Fig. 1, right side). The oxidation using $=CuCl_2$ catalyst precursor is initiated by thermal auto-oxidation of tetralin into peroxide, which "activates" the catalyst, producing =Cl–Cu–O by losing one Cl on the plane and replacing it with oxygen. Then it starts the propagation cycle that proceeds through molecules of tetralin by hydrogen bonding to the oxygen on the =ClCuO site. There the adduct suffers an intramolecular isomerization that transfers oxygen to the nuclei to produce tetralol and "reduces" the site to ClCu–(PVP). This site is reoxidized by the oxygen (molecular) to generate =ClCuOO. This structure might adsorb other TH molecules by a hydrogen bridge. Again, the intramolecular isomerization produces HOCuCl–, which restarts the catalytic cycle, producing TO, and so on. At the same time, the OCuCl– site can convert the TOH into TO and dioxygenated molecules.

Up to now, it has been clear that the reaction starts via formation of a hydroperoxide in homogeneous phase; we now describe what happens with adsorbed "peroxide" and products. To better explain this mechanism, we evaluate the catalyst characteristics before and after reaction with pure tetralin. We then discuss the potential structure of the active species that could explain the difference in activity and selectivity.

3.2. Fresh Cu/PVP catalyst characterization

The support of our Cu-catalyst is a pyridine, 4-ethenyl-polymer with diethenyl-benzene backbone (25% cross-linked) available in a spheroid shape and with a particle size of around 100–200 μm. It has an average surface area of 90 m^2/g, a particle density of 0.59 g/cm^3, a skeletal density of 1.12 g/cm^3, average pore radius of 60 nm, and a density of 0.62 g/cm^3. The study of the isothermal adsorption of $CuCl_2$ in methanol indicates a maximum adsorption capacity of 15 μmol/g. Leaching with 1 N HCl acid confirmed the amount of Cu adsorbed. Figs. 2a, 2b, and 2c depict the metal–polymer interaction (neglecting the polymer twisting of the structure), to show how the metal may be linked to the one, two, or three pyridine group. The distance between nitrogen and metal on the surface depends on the vinylbenzene–pyridine structure (blocks), as well as on the degree of cross-linking and twisting. The questions arise as to whether different metal contents might use different receptor sites that generate different links and spatial organizations, and whether this structure has different affects on the activity and selectivity of tetralin oxidation.

We start by discussing the effect of Cu in the FTIR bands of (PVP) support. Fig. 3a shows the FTIR of the (PVP) in the region of 2000–900 cm^{-1}, with adsorption bands at 1595, 1554, and 1414 cm^{-1} assigned to vibration of the pyridine rings. The adsorption bands at 1066 and 960 cm^{-1} are due to C–H bonding [22]. The main effect of adding Cu (from 0.2 to 0.45 mmol/g) was the change in the bands at 1700–1500 cm^{-1}, because the Cu ions gave a new band at 1616 cm^{-1} and a shoulder at 1635 cm^{-1}, which are assigned to pyridine–Cu bonds and to the protonated pyridine vibration. The intensity of this shoulder increased with increasing Cu^{2+} content, whereas the bands at 1598, 1555, and 1416 cm^{-1} were reduced due to the strengthened C–N bonds of the pyridine when the metal was incorporated. Figs. 3b, 3c, and 3d also show a new band at 1035 cm^{-1}, indicating a change in the asymmetric stretching vibration of the pyridine due to metal reorientation of the pyridine ring. The intensity of this band also increased with the amount of Cu^{2+}

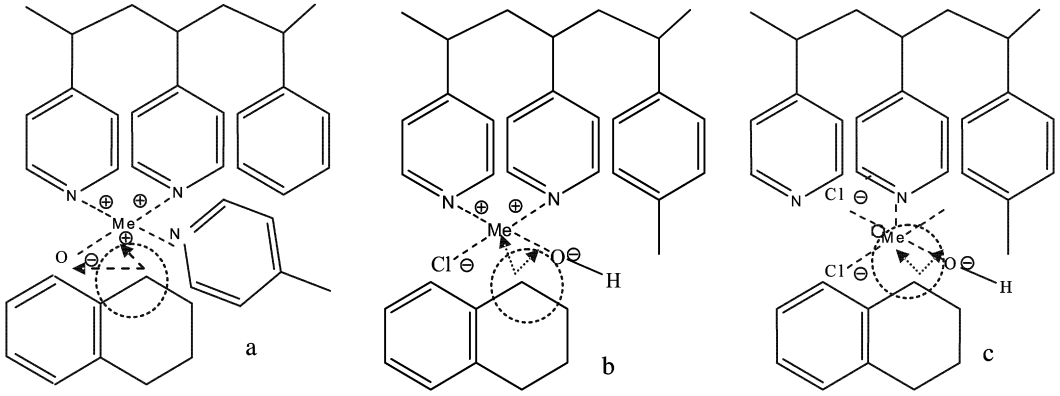

Fig. 2. Cu/(PVP) and tetralin: three a simplified schemes of interactions. (a) Three Cu–N, (b) two Cu–N, and (c) one Cu/N bondings.

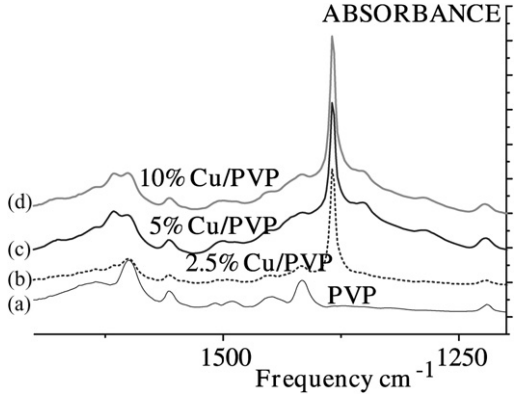

Fig. 3. FTIR: PVP (a), fresh 2.5% Cu/PVP (b), 5% Cu/PVP (c), and 10% Cu/PVP (d).

Table 1
XPS data for the 5% Cu/P(4-PVP) catalyst before and after reaction

Binding E (eV)	PVP	(F) 5% Cu/P(4-PVP)	(S) 5% Cu/P(4-PVP)
N_{1s}	399.0	399.1 and 400.3	398.2 and 400.0
$Cu_{2p3/2}$	–	933.8	932.1 and 933.8–934.0 shake up
Cu	–	512.8	511.2
Cl_{2p}	–	198.0	198.1
O_{1s}	Signals too small	Signals too small	529.4–530.4–531.1–532.0 and 533.1

in the sample. Similar results were obtained by Wu et al. [23] for $CuSO_4$/P(4-PVP).

The results of the XPS analysis are given in Table 1. The table gives the binding energy values for the main signal [24]. The (PVP) shows only one asymmetric signal at 399.1 eV assigned to N_{1s}, whereas the 5 and 10% Cu/PVP analysis indicates a broader signal of N_{1s} at around 398–400.4 eV that can be deconvoluted into two peaks. The signal at 400.3 eV is assigned to N–Cu interactions. The Cu also shows two peaks, one at 933.8 eV attributed to Cu^{2+} and another, very small peak at 512 eV due to Cu^{+}. Oxygen is not detected on (PVP) or fresh Cu/PVP. The 2.5, 5, and 10% Cu catalysts exhibit similar XPS signals, but the Cu^{2+}/Cu^{+} ratio of the signals decreases with metal content.

The ^{13}C NMR spectroscopy spectra of (PVP) and of fresh and spent 5% Cu/(PVP) samples are depicted in Fig. 4a. The (PVP) exhibits intense signals of methylene carbon C_1–C_3 and C_8–C_{11} in the range of 110–150 ppm, compared with 20–60 ppm for methyl carbon C_4–C_7 and C_{12}–C_{14}. These signals are significantly reduced in the Cu/P(4-PVP) catalyst due to an important magnetism associated with the presence of Cu^{2+} that gives a low signal/noise ratio in the spectrum obtained with polarization. In any case, qualitatively, it seems that for the low copper content catalyst, there is an important modification in the shape of carbon signal, and the loss of the signal is proportional to the Cu content in the resin.

The ^{1}H NMR spectrum for the support, depicted in Fig. 4b, shows a signal at 4.7 ppm attributed to water plus a broad signal from −5 to 8 ppm. This envelope may contain the typical signal of the 4-PVP at 6.3 and 8.4 ppm ascribed to the *ortho* and *metha* proton of the pyridine ring, and the peaks at 7, 4.3, and 0.9 attributed to aromatic methyne and methyl protons. Fig. 4b shows the spectrum of fresh 5% Cu/PVP, which exhibits an enlarged shoulder and a particular modification in the pyridine and aromatic protons.

ESR spectra for 2.5, 5, and 10% Cu/PVP samples at room temperature are plotted in Fig. 5a. All the catalysts present the axial signal with $g_{\|} > g_{\perp} > 2.03$, typical of a tetragonal Cu^{2+} d^9 environment. The $g_{\|}$ and $g_{\perp}$ values are quite similar for the 5 and 10% Cu/PVP catalyst (Table 2), as are the average $g_{\|}$ values [$g_{av} = (g_{\|} + g_{\perp}2)/3$], suggesting that the Cu^{2+} environment is very similar in these two samples. The 2.5% Cu/PVP has a slightly different environment for the Cu^{2+} ions in a more diluted catalyst. The g values in axial symmetry can be correlated by the G value, $G = (g_{\|} - 2)/(g_{\perp} - 2)$, which reflects the exchange interaction between the Cu^{2+} centers in the solid polymer complexes [25]. Thus, if $G > 4$, then the exchange interaction is negligible, whereas if $G < 4$, then the exchange interaction is significant. The G value for 2.5% Cu/PVP is 3.61, well above the values for the other two samples ($G = 2.7$ and 2.9 for 5 and 10% Cu/PVP, respectively). This finding suggests that for 2.5% of Cu contained the Cu^{2+} species is more isolated or has a longer pathway than the 5 or 10% Cu catalysts. Fig. 5 also shows the presence of a hyperfine coupling between the unpaired electron and the Cu nucleus that gives rise to four hyperfine lines in the parallel signal. These hyperfine lines are

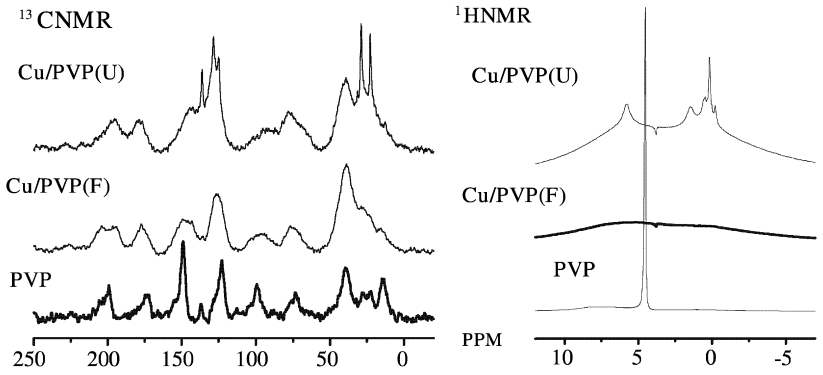

Fig. 4. Left side: ^{13}C NMR: (PVP) (a), (F) 2.5% Cu/PVP (b), (U) 5% Cu/PVP (c); right side: ^{1}H NMR: (PVP) (a), (F) 5% Cu/PVP (b), (U) 5% Cu/PVP (c).

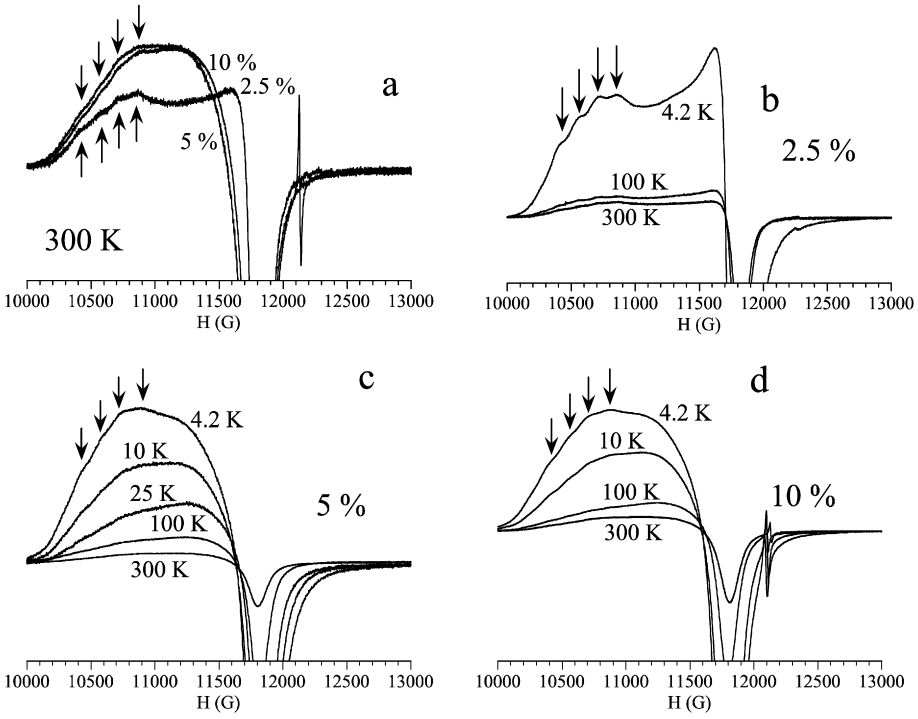

Fig. 5. (a) ESR at room temperature of the 2.5, 5, and 10% Cu/PVP samples and thermal variation of the ESR spectra of the (b) 2.5, (c) 5, and (d) 10% Cu/PVP samples. The arrows indicate the hyperfine structure of the perpendicular signal.

Table 2
ESR parameters for the 2.5, 5, and 10% Cu/PVP catalysts

Cu/PVP	$G_\perp$	$g_\parallel$	g_{av}	G	$A_\parallel$ (cm^{-1})	$g_\parallel/A_\parallel$ (cm)
2.5%	2.080	2.288	2.149	3.61	151×10^{-4}	152
5%	2.105	2.287	2.166	2.73	162×10^{-4}	141
10%	2.099	2.284	2.161	2.88	159×10^{-4}	144

more clearly observed in the 2.5% Cu/PVP (Fig. 5a) and in the low-temperature spectra (Figs. 5b, 5c, and 5d), Thus, at low temperatures, the three samples show four lines in the parallel signal [$g = 2.239(4)$, 2.274(3), 2.302(2), and 2.336(4)] also seen in Cu/PVP and picoline [25,26]. The hyperfine coupling constant (A) and the $g_\parallel/A_\parallel$ ratio are very similar for the 5 and 10% samples (Table 2), suggesting that the Cu^{2+} environments are very similar in both samples. The 2.5% Cu catalyst shows a lower $A_\parallel$ and a higher $g_\parallel/A_\parallel$ ratio (Table 2), indicating a different environment than in the two other samples. These values suggest the possibility of having in the 2.5% Cu sample a dimer Cu–Cu interaction, as was observed in Cu–pyridine studies. In fact, the $g_\parallel/A_\parallel$ parameter indicates a tetrahedral distortion of a tetragonal complex [27]. Square planar complexes present a ratio $g_\parallel/A_\parallel$ on the order of 105–135 cm, whereas ratios close to 250 cm indicate a tetrahedral distortion [27]. Our previous studies done with Cu–pyridine and Cu/PVP (not cross-linked) in CD_3OD/D_2O at 77 K indicated that this ratio changes with the Cu/Py metal/ligand ratio.

Table 2 shows that the value of $g_\parallel$ increases and that of $A_\parallel$ decreases with decreasing metal/ligand ratio, corresponding to the stepwise formation of $Cu[Py]_1$ and $Cu[Py]_4$. Detailed analysis about continuous change in ligand ratio obtained with no cross-linked pyridine can be seen in Ref. [28]. In our catalyst, as the metal content increases, the signal broadens due to dipole–dipole interactions, going from isolated centers and/or dimers

Table 3
Ratio of the I_{1616}/I_{1558} and I_{960}/I_{1598} before the reaction

Catalyst	I_{1616}/I_{1558}	I_{960}/I_{1598}
2.5% Cu/PVP	0.44	0.20
5% Cu/PVP	0.61	0.25
10% Cu/PVP	0.52	0.24

in the 2.5% Cu/PVP sample to a complex structure in the 5 and 10% Cu/PVP samples with important changes in the parallel signal.

All the previous information indicates that fresh catalyst has a large proportion of Cu^{2+} in a tetrahedral environment bonded to the surface by one or two pyridines. It presents a planar square structure of $CuCl_2$ without the presence of oxygen at detection level. The higher the metal content, the higher is the Cl on the surface and the lower the amount of "free" nitrogen. At low metal loading, this tetrahedral organization seems more distorted by the presence of a dimeric type of structure and well dispersed (lower dipole–dipole interactions) on the support than those observed at higher metal loading. Very small amounts of Cu^{+} are present in all samples, and the ratio Cu^{2+}/Cu^{+} decreases with metal content. The paper will now present what occurs after reaction with the species on surface.

3.3. Fresh-used Cu/PVP

The catalysts are contacted with tetralin and oxygen at 80 °C, washed with toluene and methanol, dried and characterized using the same methodology presented for fresh samples. During the reaction, the catalyst is exposed to the reactant (tetralin and oxygen) and the product of reactions (tetralol, tetralone, and polyoxygenates). The initial species present on the surface might be modified by the reaction. In fact, the XPS, FTIR, and ESR analyses of used catalysts present evidence of a different Cu species than in fresh 2.5, 5, and 10% Cu content samples.

It was observed that all the spent catalysts shown other bands in FTIR spectra than those bands above mentioned. They show an IR band at 2068 cm^{-1} attributed to υ_{C-O} of Cu–O–C bonds [20] and other bands in the regions 1600–1594, 1560–1554, 1497–1494, and 1418–1414 cm^{-1} assigned to aromatic C–C ring stretching vibration of the tetralin, and finally another weak signal at 3385 cm^{-1} that is assigned to O–H vibration of the adsorbed intermediaries. In a future contribution, we will discuss this band in association with the effect of intermediary molecule adsorption.

Semiquantitative FTIR analysis of the I_{1616}/I_{1558} and I_{960}/I_{1598} area ratios was done by deconvoluting the aforementioned spectra (Fig. 3). This analysis shows a nonlinear change in the ratio with the amount of copper content, following the sequence 5% ∼ 10% > 2.5% (Table 3). These results correspond to higher out-of-plane mobility and higher dipole in the 5 and 10% Cu compared with the 2.5% Cu samples. The ESR results confirm the much higher dipole–dipole interactions in the 5 and 10% Cu/PVP samples.

Raman spectroscopy confirms the presence of adsorbed material on all the samples (Fig. 6). For example, the 5% Cu/PVP

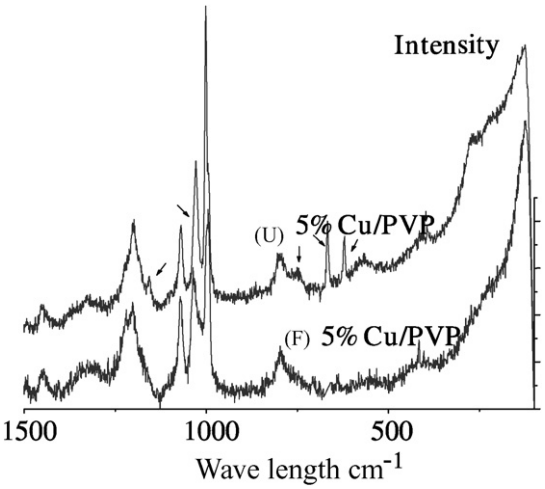

Fig. 6. Raman of fresh (F) and used (U) catalysts.

catalyst worked for 24 h, and then was washed with methanol and reused in several cycles of reaction with fresh feed to measure its activity. The arrows in Fig. 6 indicate the new Raman signals in used catalyst. The fresh catalyst shows bands at 1624 cm^{-1} (υ C=N and C=C), 1221 cm^{-1} (υ_a C–N–C), 1006 cm^{-1} (υ_a aromatics carbon), and 667 cm^{-1} (υ_a C–Cl), attributed to the pyridine ring vibrations. The increased bands at 1050 cm^{-1} and the new bands at 620 and 600 cm^{-1} indicate the presence of aromatic and oxygenated compounds on the surface. The shift of the shoulder at 280–320 cm^{-1} is probably associated with changes in the bending and stretching vibrations of Cu–pyridine with different degrees of freedom. The presence of Cu^{+} and the change in the ESR signal in the used catalyst confirm the important changes in the Cu–N active sites in used catalyst compared with fresh catalyst.

The XPS band at 933.8 eV, attributed to Cu^{2+} species, is sharper in the fresh 2.5% Cu/PVP catalyst than in the 5 and 10% Cu/PVP catalysts. The Cu signal in used catalyst is quite different because the band at 932.1 eV, assigned to Cu^{+}, is now bigger for the 5% metal-containing catalysts than for the 2.5 and 10% metal-containing catalysts. But the shake-up zone (940–933.6 eV) assigned to Cu^{2+} still is better defined in the 2.5% catalyst than in the other metal-containing catalysts. In other words, the Cu^{2+}/Cu^{+} ratio is different in the fresh catalyst than in the used catalyst. These results seem to confirm the effects of different environments in the reduction and oxidation of the Cu^{2+} ion into a Cu^{+} species by the reaction when the metal content increases and occupies "different" nitrogen positions (see the mechanism of reaction of Fig. 1). The fresh 5% CuPVP presents asymmetric, well-defined N_{1s} bands at around 398–400.4 eV, whereas the spent one exhibits an increased signal. The two peaks are shifted to 932.1 and 911 eV, respectively, by contacting the catalyst with the reaction mixture, confirming modification of the tetrahedral configuration. Calculation of the $I_N/I_{Cu^{2+}}$ and $I_N/I_{Cu^{+}}$ ratios for the three used catalysts were done using the peak intensity ratios, calibrated with Cu–polyvinylpyridine (2:1) and assuming that the transmission factor of the spectrometer and the mean free path for the electron are similar for both samples. The $N/(Cu^{2+}$ +

Table 4
Ratio of the XPS signals $I_{Cu^{2+}}/I_{Cu^{+}}$ and I_{Cl}/I_{Cu} before and after reaction

Catalyst	$I_{Cu^{2+}}/I_{Cu^{+}}$	I_O/I_{CuT}	I_{Cl}/I_{CuT}
2.5% Cu/PVP	9–4.5	0–5.1	0.9–0.8
5% Cu/PVP	6.5–4.0	0–4.8	1.4–0.9
10% Cu/PVP	7.2–4.9	0–2.2	1.9–1.2

Cu^{+}) ratio does not decrease linearly with the amount of Cu, as expected. When the copper content increases, the number of N atoms bonded to the copper ions decreases, despite the fact that the solid still has free N available for Cu adsorption (as a result of surface titration mentioned above). The square planar copper coordination with Cl is also modified by the replacement of one Cl by oxygen. By deconvolution, three oxygen signals can be identified inside the O_{1s} shoulder. These signals are attributed to O species located in some kind of square planar configuration with different levels of distortion. The relative intensities of the total oxygen change with the amount of Cu in the spent catalyst (I_O/I_{Cu} ratio) and are highest for the 2.5 and 5% Cu/PVP samples (Table 4). The changes in the Cl/Cu signals ratio are lowest for the 10% Cu catalyst, confirming the oxygen replacement in the square planar structure. Analysis is hindered by the fact that oxidized species also are adsorbed (cf. the FTIR, C NMR, and H NMR results) in spent catalyst. ^{13}C NMR spectra for spent catalyst (Fig. 4a) confirm the presence of aromatic adsorbed molecules, and ^{1}H NMR shows the presence of an important signal attributed to OH proton at 6.2 ppm. ESR analysis of spent catalyst always shows a narrowing of the Cu signal, probably due to the partial reduction of Cu^{2+} into Cu^{+}, in agreement with observations of Pomoglio and Gutrova [29] on polyethylene–polyacrylic acid.

3.4. The nature of the active phase on catalytic surface

Based on previous characterizations, we suppose that the active species are Cu^{2+} and Cu^{+} (redox system) located in a binuclear hydroxo-bridged complex formed after reaction with tetralin peroxide intermediaries. The low-concentration catalyst contains a highly dispersed species surrounded by unoccupied pyridine and located in distorted tetrahedrical position generated by helicoidally twisted (PVP) structure. The higher the Cu content, the lower the favorable coordination of the Cu with the pyridine and the lower the amount of unoccupied N surrounding the on the plane =ClCuO structure. The intercalation and twisting attributed to DVB induces two terminal pyridine groups at the extreme of each block, where only one Cu–N bond can be possible. This site, which probably is used at high Cu content (10%), also can be isolated from surrounding N species to support the adsorption of reactant and peroxides. We used a commercial sample of (PVP) with an unknown number of statistically distributed pyridine (blocks) intercalated with DVB groups, and further quantitative analysis of the results becomes difficult. Now let us consider what happens with activity (mol converted of tetralin) and selectivity (mol converted into tetralone).

3.5. Test of the active sites with tetralin

The tetralin oxidation was carried out in liquid phase without solids and in presence of silica, (PVP), (HT), Cu/HT, and Cu/PVP catalysts. Formation of TOOH was carefully measured by the phosphine method to avoid the decomposition of peroxide during the GC analysis, which might falsify the other product measurements [18], as might have occurred in some previous studies. The error in three successive analyses of pure thermal product was <0.1 wt% by weight.

3.5.1. Tetralin auto-oxidation (thermal)

Tetralin can be auto-oxidized by oxygen in its liquid phase. At 80 °C, and after an induction period, the rate of oxidation reaction is accelerated up to a certain point, and then decreased. After 24 h, the composition was 60% of TH, 10.4% of TOOH, 13.5% of TO, 5.5% of TOH, and 2.5% of Pol. During this reaction period, the amount of TOOH increased to 24%, passed through a maximum, and then decreased. The limit on the rate of tetralin conversion is apparently due to the production of a steady-state concentration of hydroperoxide formation and decomposition [29]. A tetralin conversion of 50% and a TO/TOH ratio close to 2 is achieved after 48 h of contact time, and the amount of Pol increased to 9%. The analysis of the polyoxygenates by GC–MS indicates the presence of more than 30 major compounds. Among these, we distinguished dioxygenate molecules such as 4H-benzo[d]-[1,3]dioxane, 3,4-dihydro-2H-chromene, naphthalene-1,3-(2H,4H)-dione, and naphthalene, in agreement with Kamiya et al. [30] results. We found that the higher the temperature and the residence time, the greater the Pol formation; for example, at 100 °C and 24 h of contact time, the amount of tetralin converted increases from 30 to 64% wt and amount of the polymer produced increases from 2.5 to 9.8% while the ratio one/ol remains quasi-constant (around 2). Under these conditions, the selectivity to the desired TO is poor, similar to the values reported by Mizukami et al. [31], and the amount of the heavier molecule formed makes the reaction unfeasible.

3.5.2. Effect of the presence of either homogeneous $Cu(Ac)_2$ or Cu/HT or Cu/PVP after the thermal reaction

The thermal reaction of tetralin was carried out at 80 °C for 24 h. The resulting composition was the same as described above; yields are shown in Fig. 7, left graph. Then the liquid products of the thermal reaction were contacted with different catalysts for another 8 h in a second stage of reaction. The pseudo-homogeneous $CuAc_2$ catalyst produces additional TH conversion with small changes in the TO/TH ratio and a decreased peroxide concentration. The final one/ol ratio is similar to the thermal reaction (around 2), but the product shows small increments in Pol (Fig. 1, right graph). In other words, the homogeneous Cu catalyst does not improve the selectivity to TO, despite the large amount of peroxide available at the start of the catalytic reaction, and does not control the formation of polymer.

In other tests, the products were contacted with heterogeneous Cu/HT under the same operating conditions. This cat-

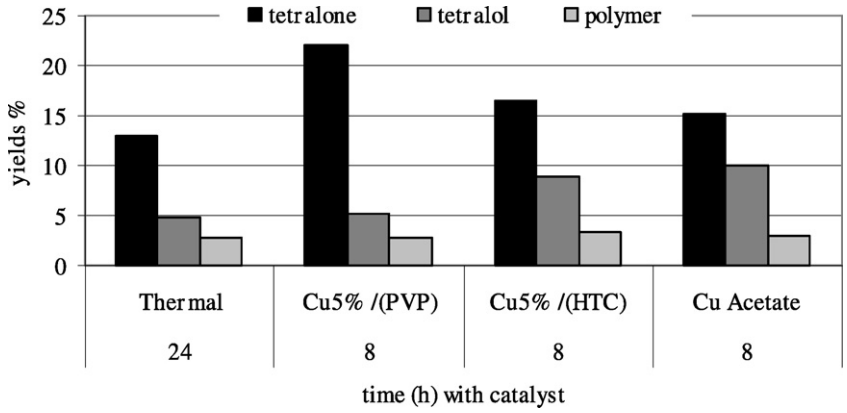

Fig. 7. Effects of catalyst on thermal product conversion (80 °C).

Table 5
Effect of PVP and catalyst on selectivity 80 °C, 12 h, 8 wt% solid

Products (wt%)	Silica	(PVP)	(HT)	$CuAc_2$	10% Cu/HT	5% Cu/PVP
Peroxide	8	0.1	3.2	4.2	3.4	1.67
Tetralin	80	98.7	95.6	84.1	86.5	86.2
Tetralone	6	2.1	0.2	6.7	7.7	9.67
Tetralol	3.3	0.1	0.09	3.33	2.8	1.29
Pol	2.6	0.0	1.2	0.5	0.4	0.1

alyst produced analogous results to those mentioned earlier for $CuAc_2$ (Fig. 1, left graph). However, the use of Cu/PVP in other tests with thermal products of reaction shows significant increases in conversion and yield in tetralone, along with a decrease in peroxide content, without increment of the Pol formed. The latter catalyst is able to direct the reaction toward the ketone and control the rate of polymer production.

3.5.3. Effects of solid (silica, (PVP), $CuAc_2$, $CuCl_2$/HT, and $CuCl_2$/(PVP)) and thermal reactions

Table 5 shows the results of TH oxidation with different catalysts operating at 80 °C for 8 h of reaction. It was demonstrated that by adding 8 g of silica (100 μm of "inert" solid) per 100 g of tetralin, the autothermal conversion was reduced from 40 to 20% and the maximum peroxide formed was reduced from 24 to 16% under the same operating conditions as those without any solid. The tests were repeated with the (PVP) varied from 2 to 8% on tetralin content. The results show a significant reduction to <1% on the maximum peroxide formed during the contact time and in those present (0.1%) at 24 h of contact. The TH conversion was around 2%, with no significant formation of Pol (Table 5). The effect of PVP on conversion and TOOH production is proportional to the amount of solid used in the range 2–5%, but above this range, the effect of incremental solid content become less and less important. FTIR analysis of the (PVP) after reaction indicates the presence of some bands of aromatics and others at 830 cm^{-1} attributed to and oxo-aromatic compound adsorbed (TOOH) on the polymer-free basic sites. This band was not proportionally decreased with the amount of PVP used in the test. That indicates another potential role of the PVP other than adsorption. Based on these results, we consider the autothermal reaction to be quasi-negligible in the presence of PVP. Taylor [7] studied the effect of polymeric surface (poly-tetra-fluoroethylene, polyethylene, and polypropylene) in tetralin auto-oxidation and found a totally opposite behavior: increased reaction rate and activation energy compared with measurements without a polymeric surface. The oxidation of TH at the same operating conditions in presence of hydrotalcite (HT), a solid with some basic properties on the surface [31], produced a increased amount of TOOH and a higher TO/TH ratio (around 2.4) compared with the values observed with silica (1.8) (Table 5). Clearly, HT has a slight effect on the control of oxidation selectivity.

The tetralin reaction is catalyzed by the presence of metal acetates (Co, Mg, Cu, Ni, and Fe [27]) with some differences in selectivity toward TO formation. In our case, the presence of a "homogeneous" Cu^{2+} catalyst directs the reaction toward the formation of a product with a one/ol ratio around 2.0 and reduces the pol formation with respect to those observed with silica. The reaction mechanism shown in Fig. 1 (left side) might be followed. Using $CuAc_2$ as catalyst for 12 h produced a 5% reduction in tetralin conversion and an 80% reduction in Pol formation compared with the values observed with pure silica, with the one/ol ratio remaining quasi-constant, around 2.0 as a function of reaction time (Table 5).

The Cu/HT might follow the mechanism 2 proposed on the right side of Fig. 1. Table 5 shows that tetralin conversion and Pol formation are, respectively, 12.6 and 7.7% lower than the values observed with (HT), whereas the ratio TO/TOH improves slightly to 2.5. The results show that the Cu/HT catalyst slightly improves the oxidation to TO via a heterogeneous mechanism, but does not control the Pol formation. The presence of a high amount of TOOH is responsible for this. After 24 h of contact time, the conversion increases slightly to 17%, but the amount of Pol formed increases to 3.7%. The higher the residence time, the lower the incremental conversion.

The Cu/PVP, which might follow the right-side mechanism presented in Fig. 1, showed a high selectivity toward TO and no appreciable Pol formation in the 24-h period. With respect to (PVP), the conversion of Cu/PVP increased from 1.3 to 13.8%, and the TO/TOH ratio was similar. After 24 h of reaction time, the conversion of TH increased to 24% and showed a continuous small reduction in the TO/TH ratio, as well as the presence of very a small amount of Pol (0.7%) in the reaction product. The amount of TOOH formed with this catalyst is always

smaller than with all other catalysts used as reference due to the effect of PVP, which depresses the thermal reaction.

3.5.4. Effect of pretreating TH with PVP followed by reaction with Cu/PVP

To check the effect of the support, a first test in TH oxidation was performed for 24 h at 80 °C with (PVP). Then the solid was removed from the reactor, the Cu/PVP catalyst was added, and the reaction was performed for 12 h. The reaction started with lower conversion and peroxide formation than in the case when the same catalyst was used with pure tetralin and without pretreatment. This delay in the catalyst activation occurs because the PVP adsorbs the "naturally occurring" peroxide, and it requires some time to form new TOOH compound. Despite this, the same selectivity was recovered after 12 h and the same conversion obtained after 24 h as for only Cu/PVP. In addition, FTIR analysis of the PVP indicates the presence of the bands at 845, 1200, 1250, 1390, and 1405 cm^{-1} attributed to –O–O– adsorbed on the surface.

3.5.5. Effects of the solid/reactant ratio (Cu/PVP/tetralin)

Fig. 8 shows the effect of the amount of catalyst on the activity and selectivity after the reactor was operated at 80 °C for 12 h using 5% $CuCl_2$/(PVP). The higher the catalyst/tetralin ratio, the higher the rate of reaction (5.67, 10.63, and 13.93% tetralin conversion) and the lower the amount of Pol observed (0.123, 0.05, and 0.02%). The TO/TOH ratio increased with the amount of catalyst between 3 and 8%, but the effect was flattened between 8 and 15%. The same effect was observed after 24 h of reaction. The reduction on Pol and peroxides are associated with the control of thermal reaction by the solid (PVP).

3.5.6. Effect of metal content

To verify the effect of the metal content, the reaction was studied at an 8% solid/tetralin ratio. Table 6 depicts the results of tetralin conversion and selectivity to products (wt%). In this case, the amount of Cu was increased from 0 to 2.5, 5, and 10 wt% with the amount of solid/tetralin kept constant; in other words, the effect of the solid content was constant. The Cu loading was well below the maximum adsorption capacity of the (PVP), the metal was "linked" with the N in the PVP, and no clusters were formed by precipitation of the salts. The catalyst characterization discussed above indicates that after reaction, the Cu–N coordination was not the same for the three metal loadings. Activity and selectivity measurements (Table 6) show that the catalyst with 2.5% Cu had the lowest conversion of TH and Pol production among the Cu-containing catalysts, but the best selectivity to TO production. The same trend was observed for 24 h of reaction. TH conversion and selectivity to TO were maximized in the 5% Cu catalyst, which also showed modest Pol formation. When the amount of free N was decreased due to the higher metal loading, both peroxide and Pol formation increased at 12 h. The maximum selectivity at 5% can be associated with the Cu^{2+}–Cu^{+} active center formed at low-coverage medium metal loading (see Table 4), which orients the reaction toward tetralone and limits the further conversion of TOH to Pol. When the highest amount of metal was added (10%), the conversion into TOOH increased, probably due to the decreased amount of nitrogen available for adsorption and the lower selectivity of additional Cu sites. The preparation of catalyst in two stages—impregnation and drying of 5% of Cu on PVP, followed by other addition of 5% of Cu—produced the same results as for those prepared in one stage with 10% Cu on PVP.

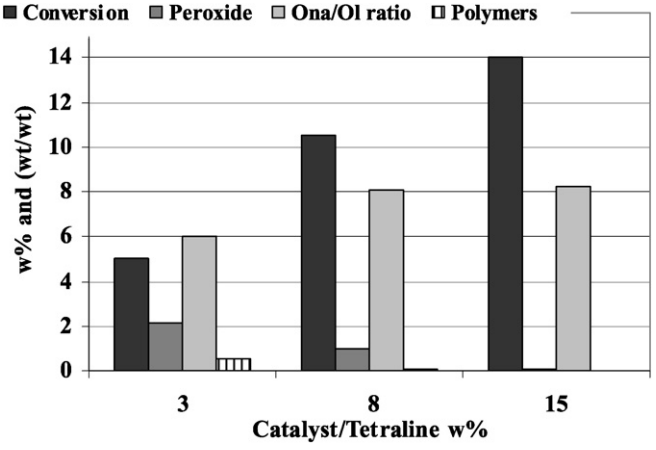

Fig. 8. Effect of the amount of catalyst used.

3.5.7. Effect of temperature

The test of the tetralin oxidation without any solid at three temperatures between 80 and 100 °C shows that the tetralin conversion increased with apparent activation energy of 15.4 kcal/mol. This is almost 2 kcal/mol higher than the values reported by Taylor [7] in a no-bubbling system using the rate of oxygen consumption instead of the tetralin conversion to calculate it. These findings indicate that the thermal one/ol ratio decreased while the amount of Pol formation increased with temperature. Using 2, 5, and 10% Cu/PVP catalysts, it can be seen that the higher the temperature, the faster the conversion of tetralin and lower the selectivity (Table 7). For both catalysts, it appeared that a small amount of Pol was formed at high temperature, indicating that the thermal reaction was still growing faster than the catalytic reaction. The activation energy for tetralin disappearance seemed to be quasi-independent of the metal content, but that for Pol formation increased with

Table 6
Effect of the amount of Cu (PVP) on activity and selectivity, (80 °C), 12 h, (%)

Catalysts	Tetral conv.	Peroxide	Tetralone	Tetralol	Pol
0% Cu/P(PVP)	7.6	0.24	6.34	0.79	0.23
2.5% Cu/P(PVP)	11.26	1.18	8.8	0.99	0.29
5% Cu/P(PVP)	12.64	1.48	7.16	1.62	1.38
10%Cu/P(PVP)	7.6	0.24	6.34	0.79	0.23

Table 7
Effects of temperature on one/ol ratio and Pol formation (wt%, 12 h)

Temperature (°C)	2.5% Cu/P(4-PVP)	5% Cu/P(4-PVP)	10% Cu/P(4-PVP)
80	9.0/0.0	7.14/0.00	5.01/0.0
90	8.0/0.0	4.9/0.05	4.2/0.1
100	6.2/0.0	4.2/0.10	3.1/0.3

the amount of Cu. For 2.5% of metal, the highest one/ol ratio was obtained at all temperatures, and still no polymer was formed. Again, the particular structure of the 2.5% Cu compared with the other catalysts seems to be responsible for the better selectivity.

3.5.8. Effect of using the same catalyst or the same product in a second run

To verify the possibility that the catalyst can be deactivated by polymer or by other product adsorption, the first 24-h run was followed by a second run performed using fresh catalyst with the product of the first run. It was observed that the fresh catalyst in the second run continued the conversion of tetralin at a lower rate and with lower selectivity to TO. In another test, the catalyst used in the first run (12 h at 80 °C) was then reused with another charge of fresh tetralin in a second run (24 h at 80 °C). The results indicate that roughly the same conversion (7.2%) was achieved and the same one/ol ratio was obtained in both runs. Clearly, the catalyst was not deactivated when working at a conversion <20%, but above that, the presence of a high concentration of product reduced the rate of reaction. These results will be analyzed in detail in a future contribution.

The tetralin oxidation mechanism in the presence of a Cu/PVP catalyst follows a complex path (Fig. 1) but seems to start with the formation of a thermal hydroperoxide (TOOH) that adsorbs and activates the catalyst. Then the tetralin molecules are adsorbed and start the oxidation cycle that forms a peroxide on surface, and the conversion into TO and TOH becomes independent of the TOOH concentration in the liquid phase because its role is minimized by the presence of the basic polymer (PVP). In this way, at low temperature, tetralin conversion occurs mainly on the surface using the O–Cu^{2+}–Cl and Cu^{+}–Cl active centers. At high temperature, the role of thermal reaction becomes important and changes the product distribution. The thermal hydroperoxide reacts with the TOH generated on the surface, producing the Pol. The catalytic test confirmed the role of the PVP in the suppression of peroxide and the control of selectivity by the surface.

4. Conclusion

Three different Cu-content catalysts anchored in a polyvinylpyridine support were characterized by different spectroscopy measurements and chemical reactions. Their performance was compared with those of homogeneous $CuAc_2$ and heterogeneous Cu/HT. Based on our findings, we can draw the following conclusions:

- The polymer itself depressed the amount of hydroperoxide formed by auto-oxidation of tetralin. The HT and the $CuAc_2$ were not able to do this.
- During the reaction of the catalyst reaction with oxygen, the initially formed or seed hydroperoxide activated the catalyst by exchanging a Cl^{-} with one O^{-} in the original $CuCl_2$ species located on the plane (in a pseudotetragonal structure) and linked to the pyridine groups. The active compounds were then reduced by tetralin and reoxidized by the molecular oxygen in a cycle independent of the peroxide content in the liquid phase. ESR, FTIR, and XPS of the used catalyst confirmed the presence of the oxygen, Cu^{2+}, and Cu^{+} species and an important modification in N–Cu interaction. The higher the metal content, the lower the coordination of the Cu with the pyridine, and the metal occupied a more distorted tetrahedrical position and thus probably was less able to perform a redox cycle during the oxidation. This finding confirmed the stability of the active structure in several cycles of reaction.
- The active phase in 2.5% Cu content (used) catalyst had a preferred organization type, (Cu^{2+} and Cu^{+})–$[Py]_2$, in a distorted tetrahedrical structure. This structure is associated with the lowest rate of tetralin oxidation and the greatest capability of producing tetralone. The increase in Cu content to 5% Cu augmented the tetralin conversion but reduced the selectivity. Adding 10% of Cu reduced both activity and selectivity, demonstrating that the use of less favorable (Cu^{2+}–Cu^{+})–$[Py]_{1-2}$ sites increased the dipole–dipole Cu interaction on the surface and reduced the amount of free nitrogen surrounding the Cu active species.
- The selectivity to tetralone and the production of polyoxygenated compounds were dependent on temperature, with lower apparent activation energy in the thermal reaction compared with the catalytic reaction. The role of homogeneous hydroperoxide in the reaction is a very important factor in the production of undesired products.

Acknowledgments

Financial support was provided by the Spanish Ministry of Education and Science (grant SAB-2003-0014). The authors thank A. Corma for valuable discussions and M. Domine for helping with the initial catalyst preparation.

References

[1] A. Corma, H. Garcia, Chem. Rev. 102 (10) (2002) 3837–3892.
[2] H. Tadokoro, S. Nishiyama, Sh. Tsuruya, M. Masai, J. Catal. 138 (1992) 24–37.
[3] M. Chanda, K. O'Driscoll, R.E. Williams, J. Mol. Catal. 7 (1980) 389–444.
[4] J.Ch. Hu, Y. Cao, P. Yang, J.-F. Deng, K.N. Fan, J. Mol. Catal. A Chem. 185 (2002) 1–9.
[5] H.C. Meinders, G. Challa, J. Mol. Catal. 7 (1980) 321–335.
[6] G. Goe, Ch. Marston, E. Scriven, E. Showers, Application of Pyridine Containing Polymers in Organic Chemistry, Prentice Hall, Englewood Cliffs, NJ, 1990, Chap. 17, pp. 275–285.
[7] W.F. Taylor, J. Catal. 16 (1970) 20–26.
[8] A. Mukhrjee, W.F. Graydon, J. Phys. Chem. 71 (13) (1967) 4232–4240.
[9] N.V. Klimova, I. Ioffe, Kinet. Katal. 8 (1967) 565–577.
[10] H. Brederec, A. Wagner, D. Glascher, K.G. Kottenhaham, Chemistry 92 (1959) 2628–2701.
[11] M. Hronec, V. Vesely, Collect. Czech. Chem. Commun. 42 (6) (1977) 1851–1858.
[12] D. Mukesh, S. Bhaduri, V. Khanwalkar, Chem. Eng. J. 41 (2) (1989) 77–84.
[13] L.J. Csanyi, K. Jaky, K. Hollosi, K. Hung, Oxid. Commun. 6 (1–4) (1984) 199–210.
[14] R.W. Coon, US Patent 4,473,711 (1984).
[15] G.L. Goe, T.D. Bailey, J.R. Beadle, US Patent 4753911 (1988).

[16] R. Galiasso Tailleur, P. Acosta, Appl. Catal. A Gen. (2006), in press.
[17] M.J. Climent, A. Corma, R. Guil-Lopez, S. Iborras, J. Primo, Catal. Lett. 59 (1999) 33–38.
[18] R. Galiasso Tailleur, G. Grendelle, S. Bercovich, Petrotecnia 15 (1977) 111–116.
[19] S. Lunak, M. Vaskova, P. Lederer, J. Veprek, J. Mol. Catal. 34 (1986) 321–324.
[20] G. Tian, D. Xia, F. Zhan, Energy Fuels 18 (2004) 49–53.
[21] B. Moden, B. Zhan, J. Dakka, J.G. Santiesteban, E. Iglesia, J. Catal. 239 (2006) 390–401.
[22] P. Hebert, A.L. Rille, W.Q. Zheng, A.J. Tadjeddine, Electroanal. Chem. 5 (1998) 447–453.
[23] K.H. Wu, Y.R. Wang, W.H. Hwu, Polym. Degrad. Stab. 79 (2003) 195–200.
[24] C. Giacomelli, F.C. Giacomelli, A. Santana, V. Schmidt, A.T. Nunes-Pires, J.R. Bettlino, A. Spinelli, Braz. J. Chem. Soc. 15 (2004) 818–822.
[25] A. Pardey, A. Rojas, J. Yanez, P. Betancourt, C. Scott, C. Chinea, C. Uribina, D. Moronta, C.I. Longo, Polyhedron 24 (2005) 511–519.
[26] H. Nishide, E. Tsuchida, J. Polym. Sci. 19 (1981) 835–837.
[27] H. Li, Y. Xu, J. Wang, L. Zhang, Polym. Prep. 44 (2) (2003) 745–746.
[28] G.M. Larin, G.V. Kolosov, G.V. Panova, K. Vikulova, Zh. Neorg. Khim. 18 (1973) 2868–2884.
[29] A.D. Pomoglio, N.D. Golubeva, J. Inorg. Organomet. Polym. 11 (2001) 67–72.
[30] Y. Kamiya, K.U. Ingold, Can. J. Chem. 42 (1964) 2424–2433.
[31] F. Mizukami, Y. Horiguchi, M. Tajima, J. Imamura, Bull. Chem. Soc. Jpn. 52 (9) (1979) 2689–2695.